5636 *Inorg. Chem.* **2009**, *48*, 5636–5647
DOI: 10.1021/ic900385y

Inorganic Chemistry
Article

New Porphyrins Bearing Positively Charged Peripheral Groups Linked by a Sulfonamide Group to *meso*-Tetraphenylporphyrin: Interactions with Calf Thymus DNA

Janet Manono, Patricia A. Marzilli, and Luigi G. Marzilli*

Department of Chemistry, Louisiana State University, Baton Rouge, Louisiana 70803

Received February 24, 2009

New water-soluble cationic *meso*-tetraarylporphyrins (TArP, Ar = 4-C_6H_4) and some metal derivatives have been synthesized and characterized. One main goal was to assess if *N*-methylpyridinium (*N*-Mepy) groups must be directly attached to the porphyrin core for intercalative binding of porphyrins to DNA. The new porphyrins have the general formula, [T($R^2R^1NSO_2Ar$)P]$X_{4/8}$ (R^1 = CH_3 or H and R^2 = *N*-Mepy-*n*-CH_2 with *n* = 2, 3, or 4; or R^1 = R^2 = $Et_3NCH_2CH_2$). Interactions of selected porphyrins and metalloporphyrins (Cu(II), Zn(II)) with calf thymus DNA were investigated by visible circular dichroism (CD), absorption, and fluorescence spectroscopies. The DNA-induced changes in the porphyrin Soret region (a positive induced CD feature and, at high DNA concentration, increases in the Soret band and fluorescence intensities) indicate that the new porphyrins interact with DNA in an outside, non-self-stacking binding mode. Several new metalloporphyrins did not increase DNA solution viscosity and thus do not intercalate, confirming the conclusion drawn from spectroscopic studies. Porphyrins known to intercalate typically bear two or more *N*-Mepy groups directly attached to the porphyrin ring, such as the prototypical *meso*-tetra(*N*-Mepy)porphyrin tetracation (TMpyP(4)). The distances between the nitrogens of the *N*-Mepy group are estimated to be ~11 Å (*cis*) and 16 Å (*trans*) for the relatively rigid TMpyP(4). For the new flexible porphyrin, [T(*N*-Mepy-4-$CH_2(CH_3)NSO_2Ar$)P]Cl_4, the distances between the nitrogens are estimated to be able to span the range from ~9 to ~25 Å. Thus, the *N*-Mepy groups in the new porphyrins can adopt the same spacing as in known intercalators such as TMpyP(4). The absence of intercalation by the new porphyrins indicates that the propensity for the *N*-Mepy group to facilitate DNA intercalation of cationic porphyrins requires direct attachment of *N*-Mepy groups to the porphyrin core.

Introduction

The ability of cationic porphyrins to associate with DNA and RNA has prompted studies of medical and biological applications of porphyrins.[1−3] Pioneering work by Fiel and co-workers demonstrating that TMpyP (*meso*-tetra(*N*-Mepy)porphyrin tetracation, *N*-Mepy = *N*-methylpyridinium group, Figure 1) has a strong affinity for DNA[3] stimulated many subsequent studies.[4−8] TMpyP(4) (having the 4-Mepy group with the pyridinium moiety linked through the 4- position) and its derivatives exhibit activity against human immunodeficiency virus, the virus responsible for AIDS.[9] TMpyP(4) has also been used in various therapeutic applications, for example, as photosensitizers in photodynamic therapy,[2,3,10−13] inhibitors of telomerase DNA cleavage,[14−16] and anticancer agents.[17,18]

*To whom correspondence should be addressed. E-mail: lmarzil@lsu.edu.

(1) Marzilli, L. G. *New J. Chem.* **1990**, *14*, 409–420.
(2) Ishikawa, Y.; Yamakawa, N.; Uno, T. *Biorg. Med. Chem.* **2007**, *15*, 5230–5238.
(3) Fiel, R. J.; Howard, J. C.; Mark, E. H.; Dattagupta, N. *Nucleic Acids Res.* **1979**, *6*, 3093–3118.
(4) Carvlin, M. J.; Dattagupta, N.; Fiel, R. J. *Biochem. Biophys. Res. Commun.* **1982**, *108*, 66–73.
(5) Carvlin, M. J.; Fiel, R. J. *Nucleic Acids Res.* **1983**, *11*, 6121–6139.
(6) Carvlin, M. J.; Mark, E.; Fiel, R.; Howard, J. C. *Nucleic Acids Res.* **1983**, *11*, 6141–6154.
(7) Fiel, R. J. *J. Biomol. Struct. Dyn.* **1989**, *6*, 1259–1275.
(8) Fiel, R. J.; Munson, B. R. *Nucleic Acids Res.* **1980**, *8*, 2835–2842.
(9) Dixon, D. W.; Schinazi, R.; Marzilli, L. G. *Ann. N.Y. Acad. Sci.* **1990**, *616*, 511–513.
(10) Bristow, C.-A.; Hudson, R.; Paget, T. A.; Boyle, R. W. *Photodiagn. Photodyn. Ther.* **2006**, *3*, 162–167.
(11) Engelmann, F. M.; Mayer, I.; Gabrielli, D. S.; Toma, H. E.; Kowaltowski, A. J.; Araki, K.; Baptista, M. S. *J. Bioenerg. Biomembr.* **2007**, *39*, 175–185.
(12) Kessel, D.; Luguya, R.; Vicente, M. G. H. *Photochem. Photobiol.* **2003**, *78*, 431–435.
(13) Munson, B. R.; Fiel, R. J. *Nucleic Acids Res.* **1992**, *20*, 1315–1319.
(14) Groves, J. T.; Farrell, T. P. *J. Am. Chem. Soc.* **1989**, *111*, 4998–5000.
(15) Han, F. X.; Wheelhouse, R. T.; Hurley, L. H. *J. Am. Chem. Soc.* **1999**, *121*, 3561–3570.
(16) Vicente, M. G. H. *Curr. Med. Chem.: Anti-Cancer Agents* **2001**, *1*, 175–194.
(17) Ding, L.; Etemad-Moghadam, G.; Cros, S.; Auclair, C.; Meunier, B. *J. Med. Chem.* **1991**, *34*, 900–906.
(18) Izbicka, E.; Wheelhouse, R. T.; Raymond, E.; Davidson, K. K.; Lawrence, R. A.; Sun, D. Y.; Windle, B. E.; Hurley, L. H.; Von Hoff, D. D. *Cancer Res.* **1999**, *59*, 639–644.

Published on Web 06/11/2009

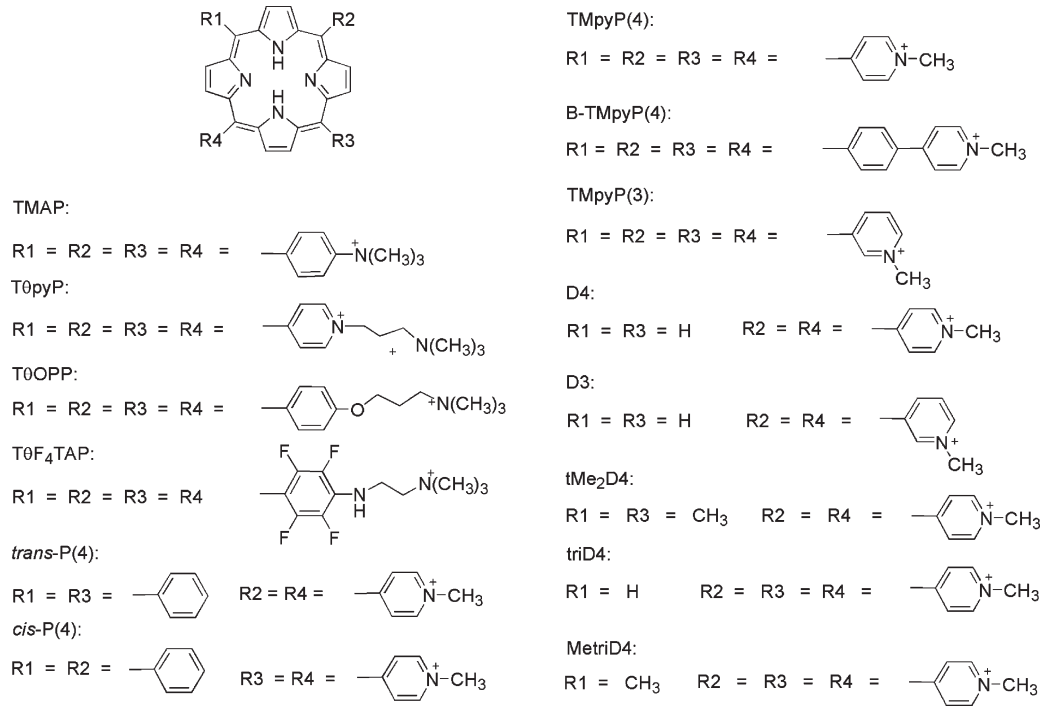

Figure 1. Structures of porphyrins mentioned in this study.

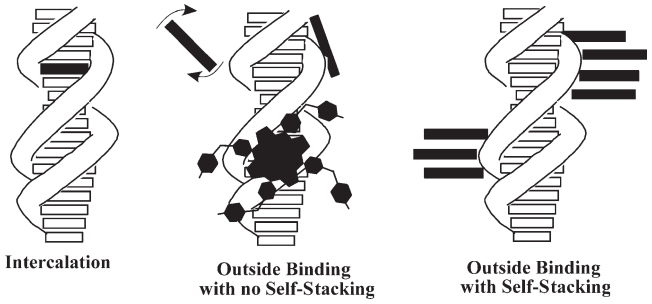

Figure 2. Binding modes of cationic porphyrins (represented by black bars in most cases). For outside binding without stacking, two subtypes are shown in the middle drawing. The upper left of this drawing illustrates how a tumbling porphyrin (shown side-on) such as TMpyP(2) might bind while its porphyrin core is maintained relatively far from the DNA. The other more commonly found subtype, shown both face-on (bottom) and side-on (upper right), allows the porphyrin core to approach the DNA more closely.

Several types of noncovalent interactions of cationic porphyrins with DNA have been found, including intercalative binding, simple outside binding, and outside binding with self-stacking (Figure 2).[5−7,19,20] The preferred binding mode and the distribution between modes are both highly dependent on the type of DNA and on the peripheral substituent groups on the porphyrin.[21,22] To achieve intercalation, the porphyrin core must have a limited thickness.[4,5,23] The metal-free porphyrin, TMpyP(4) (Figure 1), and its metal complexes constitute the porphyrin series most extensively studied for DNA binding; MTMpyP(4) with no axial ligands, such as Cu(II)TMpyP(4), generally intercalate into GC-rich DNA regions.[1,19,24] NMR spectral changes accompanying the binding of TMpyP(4) to oligodeoxyribonucleotides showed preferential insertion at the 5′-CG-3′ site.[25] An X-ray structure shows Cu(II)TMpyP(4) bound to $[d(CGATCG)]_2$ by intercalation between the C and the G of 5′-TCG-3′ accompanied by extrusion of the C of 5′-CGA-3′.[26] Metalloporphyrins possessing axial ligands, such as MTMpyP(4), with M = Fe(III), Co(III), and Zn(II), do not intercalate.[1,27] In general, these species bind preferentially to AT-rich DNA regions.[27] Water-soluble cobalt porphyrins containing a covalent axial methyl ligand synthesized in our laboratory were also found to be outside-binders with AT selectivity.[28]

In contrast to this clear understanding of how axial ligands influence intercalative versus outside binding, the influences of the properties of the peripheral group and of the electronic properties of porphyrins with a thin core were not so well understood. Porphyrins that self-stack in aqueous solution (e.g., TMAP and *cis*- and *trans*-P4, Figure 1) are preferentially outside binders,[4,5,20,29,30] and porphyrins that have a low propensity to self-stack (such as TMpyP(4), Figure 1) are intercalators.[3,31] Thus, the electron-richness of the core could

(19) Strickland, J. A.; Banville, D. L.; Wilson, W. D.; Marzilli, L. G. *Inorg. Chem.* **1987**, *26*, 3398–3406.
(20) Banville, D. L.; Marzilli, L. G.; Strickland, J. A.; Wilson, W. D. *Biopolymers* **1986**, *25*, 1837–1858.
(21) Pasternack, R. F.; Gibbs, E. J.; Villafranca, J. J. *Biochemistry* **1983**, *22*, 2406–2414.
(22) Gray, T. A.; Yue, K. T.; Marzilli, L. G. *J. Inorg. Biochem.* **1991**, *41*, 205–219.
(23) Pasternack, R. F.; Gibbs, E. J.; Villafranca, J. J. *Biochemistry* **1983**, *22*, 5409–5417.
(24) Pasternack, R. F.; Gibbs, E. J.; Gaudemer, A.; Antebi, A.; Bassner, S.; Depoy, L.; Turner, D. H.; Williams, A.; Laplace, F.; Lansard, M. H.; Merienne, C.; Perreefauvet, M. *J. Am. Chem. Soc.* **1985**, *107*, 8179–8186.
(25) Marzilli, L. G.; Banville, D. L.; Zon, G.; Wilson, W. D. *J. Am. Chem. Soc.* **1986**, *108*, 4188–4192.
(26) Lipscomb, L. A.; Zhou, F. X.; Presnell, S. R.; Woo, R. J.; Peek, M. E.; Plaskon, R. R.; Williams, L. D. *Biochemistry* **1996**, *35*, 2818–2823.
(27) Ward, B.; Skorobogaty, A.; Dabrowiak, J. C. *Biochemistry* **1986**, *25*, 7827–7833.
(28) Trommel, J. S.; Marzilli, L. G. *Inorg. Chem.* **2001**, *40*, 4374–4383.
(29) Gibbs, E. J.; Tinoco, I.; Maestre, M. F.; Ellinas, P. A.; Pasternack, R. F. *Biochem. Biophys. Res. Commun.* **1988**, *157*, 350–358.
(30) Pasternack, R. F.; Bustamante, C.; Collings, P. J.; Giannetto, A.; Gibbs, E. J. *J. Am. Chem. Soc.* **1993**, *115*, 5393–5399.

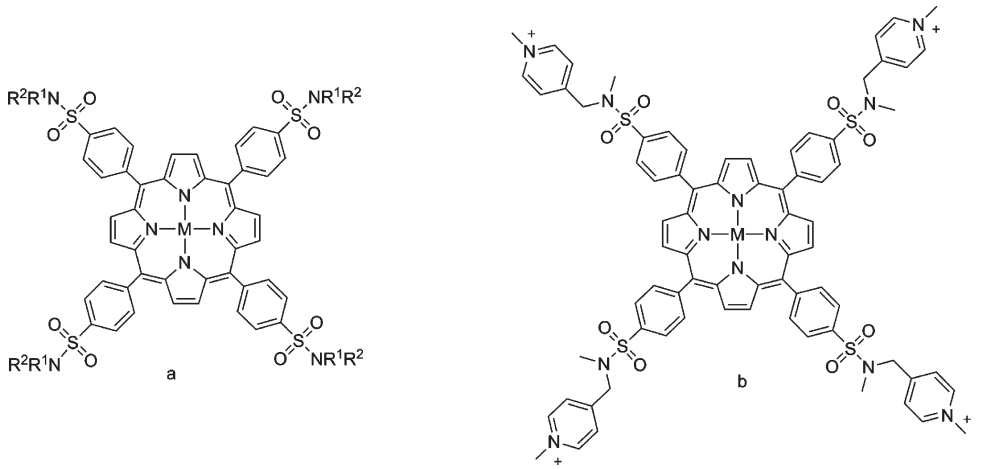

Figure 3. Structures of new porphyrins: (a) $[MT(R^2R^1NSO_2Ar)P]X_{4/8}$ (in **1** to **3**, M = 2H and R^1 = H and R^2 = *N*-Mepy-*n*-CH_2, with *n* = 2, 3, or 4, respectively; in **4**, M = 2H and R^1 = H and R^2 = $Me_3NCH_2CH_2$; **5** differs from **1** in that R^1 = CH_3; in **7** and Cu(II)**7**, R^1 = R^2 = $Et_3NCH_2CH_2$ and M = 2H and Cu(II), respectively; and (b) $[MT(N\text{-Mepy-4-}CH_2(CH_3)NSO_2Ar)P]Cl_4$ (in **6**, M = 2H; in Cu(II)**6**, M = Cu(II); and in Zn(II)**6**, M = Zn(II)).

possibly stabilize the self-stacked, outside-bound porphyrin-DNA adduct, disfavoring intercalation.[32] To probe the influence of porphyrin properties on the DNA binding modes, we previously investigated the tentacle porphyrins depicted and defined in Figure 1. These studies revealed that only porphyrins possessing *N*-alkylated pyridinium groups, such as T*θ*pyP, intercalate into GC-rich regions of DNA.[31] In contrast, T*θ*F_4TAP and T*θ*OPP, which are similar in size and shape to T*θ*pyP but with no *N*-alkylated pyridinium groups, self-stacked along the DNA backbone and did not intercalate into DNA.[31−34] The studies with tentacle porphyrins thus indicated that, while the influence of porphyrin electron richness on the binding mode of relatively thin porphyrins was not important, pyridinium groups appear to be necessary for intercalation. Furthermore, bulk and thickness of the *N*-alkyl groups attached to the pyridinium groups but projecting away from the porphyrin core do not appear to prevent intercalation.

Taking a different tack, McMillin et al. have been synthesizing less sterically demanding porphyrins having less bulk at the periphery; these investigators have found that relatively small porphyrins such as D4 and D3 (Figure 1) intercalate into B-form DNA, regardless of the base composition.[35,36] In another study from the McMillin laboratory, the newly synthesized tMe_2D4 (Figure 1) was found to intercalate into DNA, in contrast to reports on *trans*-P(4), which binds externally, forming long-range stacked structures.[29,30,37] In a recent study of the binding modes of two tricationic porphyrins having different steric size, McMillin et al. found that triD4 (Figure 1) intercalates into $[poly(dA\text{-}dT)]_2$ ((poly dA-dT)-(poly dA-dT)), whereas the larger MetriD4 (Figure 1) binds externally, indicating that the presence of a fourth substituent destabilizes the intercalated form.[38] In summary, the size of porphyrins with *N*-alkylpyridinium groups influences the extent of intercalation in GC and AT regions.

In typical porphyrin intercalators, the *N*-alkylpyridinium group is attached to the porphyrin core, creating a common structural unit. This direct attachment allows the positive charges to delocalize onto the porphyrin ring[39] and also restricts the distances between the pyridinium groups. We now take an approach different from that of McMillin et al. and also from that we used previously. In particular, we expand the size of the pyridinium-containing porphyrins by placing a linking group between the porphyrin core and the pyridinium group. The larger but flexible porphyrins used here can assume conformations such that the separations between the charge-bearing nitrogens of the *N*-Mepy groups encompass the distances [~11 Å (*cis*) and ~16 Å (*trans*)] between these nitrogens in known intercalators. Specifically, we describe here the synthesis of new porphyrins ($[T(R^2R^1NSO_2Ar)P]X_{4/8}$) and metalloporphyrins ($[MT(R^2R^1NSO_2Ar)P]X_{4/8}$) bearing positively charged, peripheral *N*-Mepy or quaternary ammonium groups. These groups are linked to the 4-position of the phenylene group of the porphyrin by secondary ($-SO_2NHR$) or tertiary ($-SO_2NR_2$) sulfonamide groups (Figure 3).[40] These porphyrins were designed by us to determine whether the new porphyrins containing *N*-Mepy groups would be intercalators and whether the new porphyrins lacking *N*-Mepy groups would allow us to gain some insight into factors that might influence outside binding interactions. The latter type of new porphyrins also serve as appropriate controls for comparison to the new porphyrins containing *N*-Mepy groups. We investigated the calf thymus (CT) DNA binding interactions of selected porphyrins by visible CD and other spectroscopic methods. We also assessed DNA binding of several new metalloporphyrins ($[MT(R^2R^1NSO_2Ar)P]X_{4/8}$) by viscometric methods.

(31) Marzilli, L. G.; Petho, G.; Lin, M. F.; Kim, M. S.; Dixon, D. W. *J. Am. Chem. Soc.* **1992**, *114*, 7575–7577.
(32) McClure, J. E.; Baudouin, L.; Mansuy, D.; Marzilli, L. G. *Biopolymers* **1997**, *42*, 203–217.
(33) Mukundan, N. E.; Petho, G.; Dixon, D. W.; Kim, M. S.; Marzilli, L. G. *Inorg. Chem.* **1994**, *33*, 4676–4687.
(34) Mukundan, N. E.; Petho, G.; Dixon, D. W.; Marzilli, L. G. *Inorg. Chem.* **1995**, *34*, 3677–3687.
(35) Bejune, S. A.; Shelton, A. H.; McMillin, D. R. *Inorg. Chem.* **2003**, *42*, 8465–8475.
(36) Wall, R. K.; Shelton, A. H.; Bonaccorsi, L. C.; Bejune, S. A.; Dube, D.; McMillin, D. R. *J. Am. Chem. Soc.* **2001**, *123*, 11480–11481.
(37) Shelton, A. H.; Rodger, A.; McMillin, D. R. *Biochemistry* **2007**, *46*, 9143–9154.
(38) Andrews, K.; McMillin, D. R. *Biochemistry* **2008**, *47*, 1117–1125.
(39) Kano, K.; Minamizono, H.; Kitae, T.; Negi, S. *J. Phys. Chem. A* **1997**, *101*, 6118–6124.
(40) Manono, J.; Marzilli, P. A.; Fronczek, F. R.; Marzilli, L. G. *Inorg. Chem.* **2009**, DOI: 10.1021/ic900600z.

Experimental Section

Materials and Methods. All compounds and reagents used in the synthetic chemistry were purchased from Aldrich. The chloride salts of Cu(II)TMpyP(4) and Cu(II)TMAP were obtained from MidCentury. The syntheses of the non-alkylated porphyrin precursors are described elsewhere.[40] The mean length of the DNA was ~5000 bp, established by gel electrophoresis on 1% agarose gel.[41] All CT DNA solutions were stored at −20 °C and were allowed to warm to room temperature (RT) before sample preparation. Stock solutions of CT DNA (GE Amersham) were prepared in 10 and 100 mM NaCl at pH 7.0. The CT DNA concentration in base pairs was determined by UV spectroscopy by using $\varepsilon_{260} = 1.32 \times 10^4$ M^{-1} cm^{-1}.[42] To compare our results to those of previous studies,[33,34] the porphyrin concentration was 7.5 μM in titration studies employing visible absorption, fluorescence, and CD spectroscopies.

All ^{1}H NMR spectra were recorded on either a 300 or a 400 MHz Bruker NMR spectrometer. Peak positions are relative to TMS or solvent residual peak, with TMS as reference. Visible absorption experiments were performed with a Cary 3 UV−visible spectrophotometer. CD spectra and titrations were recorded at 25 °C with a Jasco 710 spectrophotometer. Fluorescence studies were performed on a Fluorolog-3 spectrofluorimeter (Horiba Jobin Yvon) at 25 °C. Excitation wavelengths were 412 nm in the absence of DNA and 422 nm in the presence of DNA. Mass spectra for samples dissolved in methanol were obtained at the Mass Spectrometry Facility at LSU on a Hitachi MS-8000 3DQ LC-ion trap ESI mass spectrometer.

Solutions for visible spectroscopy were prepared by diluting a 25 μL aliquot of 1.5 mM porphyrin stock solution in 5.0 mL of a 10 or 100 mM NaCl solution. An aliquot of CT DNA was then added to such dilute porphyrin solutions to obtain the desired value of R ([porphyrin]/[DNA base pairs]). The pH of the solution was measured and readjusted to 7.0 with 0.01 M NaOH or 0.01 M HCl before recording spectra.

Viscosity Studies. Viscosity titrations were performed by using a Cannon-Ubbelohde semi-microdilution capillary viscometer in a circulating water bath maintained at 30.5 °C. Buffer (1.0 mL of 100 mM NaCl at pH 7.0) was added to the viscometer, and the flow time was measured. Solution viscosity was determined by adding a small aliquot of CT DNA stock solution to a vial containing the buffer (~1 mL) to make the final concentration 75 μM in base pairs, and the pH was adjusted to 7.0. The flow time of the DNA solution was then obtained. An aliquot of the porphyrin stock solution (75 μM dissolved in CT DNA 75 μM) was then added to the viscometer in increments of 25 μL to give the desired value of R, while keeping the DNA concentration constant. Flow time measurements, obtained with a timer accurate to ±0.01 s, were recorded until three consecutive readings differed by less than ±0.1 s. The solution reduced viscosity (SRV) was presented as η/η_0 versus R, where $\eta/\eta_0 = t_c - t_0/t_D - t_0$ and t_0 is the flow time of the buffer, t_D is the flow time of the DNA in buffer, and t_c is the flow time of the DNA solution containing porphyrin.[43]

Competitive Binding Experiments. Solutions of Cu(II)TMpyP (4) (75 μM) and Cu(II)**6** (75 μM, Figure 3), both dissolved in 75 μM CT DNA, were prepared separately. Equal volumes of the two solutions were mixed and allowed to equilibrate for 1 h at room temperature. Aliquots of this 1:1 mixture were used as described above for viscosity measurements at different R values (where the porphyrin concentration equals the sum of the concentrations of the two Cu(II) porphyrins).

Sodium Dodecyl Sulfate (SDS) Studies. SDS solutions were prepared by adding surfactant in water (e.g., for 1 M SDS (2.89 g) in 10 mL) and stirring for 15 min, when the solution became clear. An aliquot of the desired porphyrin stock solution (1.5 mM) was added to make a 7.5 μM solution, the pH was adjusted to 7.0, and the visible spectral changes were monitored with time. In one experiment, an aliquot of the porphyrin stock solution was diluted with water to 15 μM. After ~10 min this solution was added to an equal volume of a 2 M SDS solution such that the final concentrations were 1 M SDS and 7.5 μM porphyrin. The pH was quickly readjusted to 7.0, and the visible spectrum recorded.

General Synthesis for Alkylated [T($R^2R^1NSO_2Ar$)P]X_4 Porphyrins 1 to 6. Alkylation was carried out by suspending the parent porphyrin in an excess of CH_3I (10 mL) in a sealed flask and allowing the mixture to stir at RT overnight. The CH_3I that did not react was allowed to evaporate; the residue was dried under vacuum for 3 h to yield the iodide salt of the product porphyrin. To prepare the chloride salt of porphyrins **1** to **6**, a Dowex-1 (chloride form) anion-exchange resin column was prewashed with 0.1 N HCl and then washed with water until the eluate was at pH 7.0; a slurry of the compound in water was made with the resin and loaded onto a short column, and then eluted with water. The water was removed by rotary evaporation, and the purplish solid residue dried under vacuum. The product was obtained as a purple powder by dissolving it in methanol and adding ethyl acetate. All compounds were isolated as chloride salts and analyzed by ^{1}H NMR spectroscopy and mass spectrometry.

[T(*N*-Mepy-2-CH_2(H)NSO_2Ar)P]Cl_4 (1). The general methylation method applied to the *non-alkylated* parent porphyrin (0.12 g, 0.092 mmol) afforded **1** as a brown precipitate (0.115 g, 84% yield). ^{1}H NMR (ppm) in DMSO-d_6: 8.90 (8H, s, β-pyrrole), 9.36 (4H, br, NH-sulfonamide), 9.12 (4H, d, pyH), 8.71 (4H, t, pyH), 8.49 (8H, d, ArH), 8.36 (8H, d, ArH), 8.31 (4H, d, pyH), 8.14 (4H, t, pyH), 4.87 (8H, d, CH_2), 4.44 (12H, s, CH_3), −2.95 (2H, br, NH). UV−vis (methanol) λ_{max} (ε) [nm (M^{-1} cm^{-1})]: 416 (296,100), 512 (13,600), 546 (5300), 588 (4100), 642 (2300). ESI-MS(m/z): $[M + 3H]^{3+}$ = 451.1344, $[M + 4H]^{4+}$ = 338.6032, calcd. for $[M + 3H]^{3+}$ = 451.1466, $[M + 4H]^{4+}$ = 338.5996.

[T(*N*-Mepy-3-CH_2(H)NSO_2Ar)P]Cl_4 (2). The general method using the *non-alkylated* parent (0.12 g, 0.092 mmol) afforded **2** as a brown precipitate (0.13 g, 96% yield). ^{1}H NMR (ppm) in DMSO-d_6: 8.87 (8H, s, β-pyrrole), 9.46 (4H, t, NH-sulfonamide), 9.30 (4H, s, pyH), 9.08 (4H, t, pyH), 8.72 (4H, d, pyH), 8.45 (8H, d, ArH), 8.32 (8H, d, ArH), 8.24 (4H, t, pyH), 4.57 (8H, d, CH_2), 4.42 (12H, s, CH_3), −2.96 (2H, br, NH). UV−vis (methanol) λ_{max} (ε) [nm (M^{-1} cm^{-1})]: 416 (292,800), 512 (14,000), 546 (5800), 588 (4400), 642 (2300). ESI-MS(m/z): $[M + 2H]^{2+}$ = 676.7088, $[M+3H]^{3+}$=451.1423, $[M+4H]^{4+}$ = 338.6103, calcd. for $[M + 2H]^{2+}$ = 677.1994, $[M + 3H]^{3+}$ = 451.1466, $[M + 4H]^{4+}$ = 338.5996.

[T(*N*-Mepy-4-CH_2(H)NSO_2Ar)P]Cl_4 (3). The general method using the *non-alkylated* parent (0.12 g, 0.092 mmol) afforded **3** as a brown precipitate (0.12 g, 89% yield). ^{1}H NMR (ppm) in DMSO-d_6: 8.89 (8H, s, β-pyrrole), 9.20 (4H, br, NH-sulfonamide), 9.02 (8H, d, pyH), 8.49 (8H, d, ArH), 8.32 (8H, d, ArH), 8.20 (8H, d, pyH), 4.68 (8H, d, CH_2), 4.35 (12H, s, CH_3), −2.94 (2H, br, NH). UV−vis (methanol) λ_{max} (ε) [nm (M^{-1} cm^{-1})], 416 (312,200), 512 (13,500), 546 (5200), 588 (4000), 642 (1700). ESI-MS(m/z): $[M + H]^{+}$ = 1354.4043, $[M + 2H]^{2+}$ = 676.2131, $[M + 3H]^{3+}$ = 451.14, $[M + 4H]^{4+}$ = 338.6097, calcd. for $[M + H]^{+}$ = 1354.3987, $[M +2H]^{2+}$ = 677.1994, $[M + 3H]^{3+}$ = 451.1466, $[M + 4H]^{4+}$ = 338.5996.

[T($Me_3NCH_2CH_2$(H)NSO_2Ar)P]Cl_4 (4). The general method using the *non-alkylated* parent (0.12 g, 0.099 mmol) afforded **4** as a reddish precipitate (0.095 g, 69% yield). ^{1}H NMR (ppm) in DMSO-d_6: 8.88 (8H, s, β-pyrrole), 8.69 (4H, t, NH-sulfonamide),

(41) Schaffer, H. E.; Sederoff, R. R. *Anal. Biochem.* **1982**, *115*, 113–122.
(42) Wells, R. D.; Larson, J. E.; Grant, R. C.; Shortle, B. E.; Cantor, C. R. *J. Mol. Biol.* **1970**, *54*, 465–497.
(43) Satyanarayana, S.; Dabrowiak, J. C.; Chaires, J. B. *Biochemistry* **1992**, *31*, 9319–9324.

8.48 (8H, d, ArH), 8.32 (8H, d, ArH), 3.63 (8H, d, CH_2), 3.58 (8H, t, CH_2), 3.23 (36H, s, CH_3), −2.94 (2H, br, NH). UV−vis (methanol) λ_{max} (ε) [nm (M^{-1} cm^{-1})]: 416 (266,000), 512 (12,100), 546 (5000), 588 (3800), 642 (1800). ESI-MS(m/z): $[M + 4H]^{4+}$ = 318.6365; calcd for $[M + 4H]^{4+}$ = 318.6309.

[T(*N*-Mepy-2-$CH_2(CH_3)NSO_2Ar$)P]Cl_4 (5). The general method using the *non-alkylated* parent (0.116 g, 0.086 mmol) afforded **5** as a brown precipitate (0.125 g, 93% yield). ^{1}H NMR (ppm) in DMSO-d_6: 8.98 (8H, s, β-pyrrole), 9.18 (4H, d, pyH), 8.58 (8H, d, ArH), 8.42 (8H, d, ArH), 8.74 (4H, t, pyH), 8.31 (4H, d, pyH), 8.16 (4H, t, pyH), 5.14 (8H, s, CH_2), 4.46 (12H, s, CH_3), 3.08 (12H, s CH_3), −2.81 (2H, br, NH). UV−vis (methanol) λ_{max} (ε) [nm (M^{-1} cm^{-1})]: 416 (359,600), 512 (16,700), 546 (6900), 588 (6400), 642 (2500). ESI-MS(m/z): $[M + 4H]^{4+}$ = 352.6276; calcd for $[M + 4H]^{4+}$ = 352.6177.

[T(*N*-Mepy-4-$CH_2(CH_3)NSO_2Ar$)P]Cl_4 (6). The general method using the *non-alkylated* parent (0.108 g, 0.079 mmol) afforded **6** as a brown precipitate (0.11 g, 88% yield). ^{1}H NMR (ppm) in DMSO-d_6: 8.88 (8H, s, β-pyrrole, 9.04 (8H, d, pyH), 8.56 (8H, d, ArH), 8.36 (8H, d, ArH), 8.19 (8H, d, pyH), 4.87 (8H, s, CH_2), 4.38 (12H, s, CH_3), 3.04 (12H, s, CH_3), −2.93 (2H, br, NH). UV−vis (methanol) λ_{max} (ε) [nm (M^{-1} cm^{-1})]: 416 (302,100), 512 (14,500), 546 (6000), 588 (4400), 642 (2400). ESI-MS(m/z): $[M + 4H]^{+4}$ = 352.6199; calcd for $[M + 4H]^{4+}$ = 352.6177.

[T($Et_3NCH_2CH_2$)$_2NSO_2Ar$)P]Cl_8 (7). Porphyrin **7** was synthesized from its *non-alkylated* precursor (synthesized by treating a suspension of $TPPSO_2Cl$ (0.22 g, 0.22 mmol) in acetonitrile (20 mL) with *N,N,N′,N″*-Et_4dien (0.199 g, 0.93 mmol) in acetonitrile (10 mL) at RT). The resulting suspension became a solution when stirred overnight, and the solvent was then removed by rotary evaporation. The residue was recrystallized from dichloromethane and hexane as purple crystals (0.35 g, 93% yield). ^{1}H NMR (ppm) in $CDCl_3$: 8.79 (8H, s, β-pyrrole), 8.36 (8H, d, ArH), 8.28 (8H, d, ArH), 3.55 (16H, t, CH_2), 2.84 (16H, t, CH_2), 2.67 (32H, m. CH_2), 1.12 (48H, m, CH_3), −2.84 (2H, br, NH). The non-alkylated precursor (0.13 g) was alkylated by using iodoethane (5 mL) instead of iodomethane in the procedure above, and **7** was obtained as the chloride salt (0.115 g, 89% yield) as described above. ^{1}H NMR (ppm) in DMSO-d_6: 8.95 (8H, s, β-pyrrole), 8.51 (16H, d, ArH), 4.0 (16H, t, CH_2), 3.68 (16H, t, CH_2), 3.48 (48H, s. CH_2), 1.32 (72H, m, CH_3), −2.84 (2H, br, NH). UV−vis (methanol) λ_{max} (ε) [nm (M^{-1} cm^{-1})]: 416 (320,000), 512 (15,500), 546 (6600), 588 (5100), 642 (2700). ESI-MS(m/z): $[M + 4H]^{+4}$ = 492.7939; calcd for $[M + 4H]^{4+}$ = 492.8223.

[Cu(II)T(*N*-Mepy-4-$CH_2(CH_3)NSO_2Ar$)P]Cl_4 (Cu(II)6). A solution of **6** (0.05 g, 0.032 mmol) in methanol (10 mL) was treated with copper(II) acetate (0.64 mg, 0.032 mmol) in MeOH (5 mL). The solution was allowed to stir at RT for about 1 h. Completion of the reaction was indicated by UV/vis spectroscopy, with the four Q bands of the free base (λ = 512, 546, 588, 642 nm) collapsing to one peak (λ = 538 nm). The volume of the reaction mixture was reduced to ~1 mL, and acetone was added to precipitate the compound as a red powder (0.045 g, 88% yield). ^{1}H NMR (ppm) in DMSO-d_6: 8.99 (8H, br, pyH), 8.12 (8H, br, pyH), 4.80 (8H, br, CH_2), 4.35 (12H, s, CH_3), 2.95 (12H, br, CH_3). UV−vis (methanol) λ_{max} (ε) [nm (M^{-1} cm^{-1})]: 414 (364,400), 538 (1740).

[Cu(II)T($Et_3NCH_2CH_2$)$_2NSO_2Ar$)P]Cl_8 (Cu(II)7). This compound was synthesized and isolated as for Cu(II)**6** above from (0.05 g, 0.022 mmol) of **7**; yield = 0.039 g (76%), UV−vis (methanol) λ_{max} (ε) [nm (M^{-1} cm^{-1})]: 414 (449,000), 538 (21,600).

[Zn(II)T(*N*-Mepy-4-$CH_2(CH_3)NSO_2Ar$)P]Cl_4 (Zn(II)6). A solution of porphyrin **6** (0.05 g, 0.032 mmol) in dichloromethane (10 mL) was treated with a solution of zinc acetate (0.035 g, 0.16 mmol in methanol, 2 mL). The solution was stirred at RT for 2 h, after which a small sample of the reaction mixture that was analyzed by visible spectroscopy indicated that the metal insertion was complete, with the four Q bands of the free base (λ = 514, 549, 590, 643 nm) collapsing to two peaks (λ = 556, 596 nm). The dichloromethane was removed by rotary evaporation, and the purple precipitate that formed was collected on a filter and washed with methanol to remove the excess of zinc acetate, affording the zinc complex of the precursor of porphyrin **6** (0.033 g, 63% yield). ^{1}H NMR (ppm) in DMSO-d_6: 8.85 (8H, s, β-pyrrole, 8.64 (8H, d, pyH), 8.46 (8H, d, ArH), 8.28 (8H, d, ArH), 7.46 (8H, d, pyH), 4.55 (8H, d, CH_2), 2.93 (12H, s, CH_3). The general method of alkylation described above afforded Zn(II)**6** as a purple powder (0.035 g, 93% yield). ^{1}H NMR (ppm) in DMSO-d_6: 8.85 (8H, s, β-pyrrole, 9.03 (8H, d, pyH), 8.50 (8H, d, ArH), 8.33 (8H, d, ArH), 8.20 (8H, d, pyH), 4.87 (8H, d, CH_2), 4.38 (12H, d, CH_3), 2.94 (12H, s, CH_3). UV−vis (methanol) λ_{max} (ε) [nm (M^{-1} cm^{-1})]: 424 (388,100), 556 (14,600), 596 (5,900).

Results

Synthesis. The use of various metal salts to metalate porphyrins containing a secondary sulfonamide generally produced insoluble materials. The fact that sulfonamides are known to coordinate to metal ions through both the sulfonyl oxygen and the deprotonated sulfonamide nitrogen[44,45] led us to investigate the synthesis of the porphyrins containing a tertiary sulfonamide group. Utilizing the N-Me group in place of the dissociable NH group allowed us to prepare porphyrins that are very soluble in organic solvents; this property permitted successful alkylation and metalation of the porphyrins. The cationic porphyrins ($[T(R^2R^1NSO_2Ar)P]X_{4/8}$) (Figure 3) were characterized by mass spectrometry (ESI), UV−vis (methanol), and ^{1}H NMR spectra (in DMSO-d_6). All compounds completely dissolved in suitable solvents and gave ^{1}H NMR spectra indicating the presence of only one species having signals with shifts and intensity (by integration) consistent with our formulation.

The Cu(II) complexes of the cationic porphyrins (Figure 3) were characterized by visible spectroscopy, and the Zn(II) complexes were characterized by both ^{1}H NMR and visible spectroscopy. Upon Cu(II) insertion into [T(*N*-Mepy-4-$CH_2(CH_3)NSO_2Ar$)P]Cl_4 (**6**) to form [Cu(II)T(*N*-Mepy-4-$CH_2(CH_3)NSO_2Ar$)P]Cl_4 (Cu(II)**6**), the Soret band maximum (λ_{So}) was blue-shifted by 3 nm for **6** and the number of Q bands decreased from four to one, results consistent with reported observations for other copper porphyrins, such as CuTMAP.[46,47] Zn(II) insertion into **6** to form [Zn(II)T(*N*-Mepy-4-$CH_2(CH_3)NSO_2Ar$)P]Cl_4 (Zn(II)**6**) produced a 10 nm red shift of λ_{So}, and the number of Q bands decreased from four to two; both features have been observed previously with other zinc porphyrins.[47,48]

Solution Studies with No DNA Present. Values of λ_{So} and molar absorptivity at that wavelength (ε_{So}) are summarized for several new porphyrins and for Cu(II) TMAP in Table 1. All solution studies employed 7.5 μM porphyrin and pH 7.0, unless stated otherwise. Compared

(44) Christoforou, A. M.; Fronczek, F. R.; Marzilli, P. A.; Marzilli, L. G. *Inorg. Chem.* **2007**, *46*, 6942–6949.
(45) Saladini, M.; Iacopino, D.; Menabue, L. *J. Inorg. Biochem.* **2000**, *78*, 355–361.
(46) Butje, K.; Nakamoto, K. *Inorg. Chim. Acta* **1990**, *167*, 97–108.
(47) Spellane, P. J.; Gouterman, M.; Antipas, A.; Kim, S.; Liu, Y. C. *Inorg. Chem.* **1980**, *19*, 386–391.
(48) Kalyanasundaram, K. *Inorg. Chem.* **1984**, *23*, 2453–2459.

Table 1. Visible Spectroscopic Data for [T(*N*-Mepy-4-$CH_2(CH_3)NSO_2Ar$)P]Cl_4 (**6**), Cu(II)**6**, Zn(II)**6**, Cu(II)**7**, and Cu(II)TMAP

	λ_{So}[b] ($10^{-5} \times \varepsilon_{So}$)[c]			
porphyrin[a]	in H_2O	in 10 mM NaCl	in 100 mM NaCl	in methanol
6	413 (1.5)	412 (1.1)	404 (0.9)	415 (3.0)
Cu(II)**6**	410 (2.0)	406 (1.6)	403 (1.1)	414 (3.6)
Zn(II)**6**	423 (2.9)	423 (1.8)	423 (1.5)	424 (3.9)
Cu(II)**7**	414 (3.1)	414 (2.3)	409 (2.2)	414 (4.4)
Cu(II)TMAP	411 (2.8)	411 (2.8)	411 (2.6)	412 (2.9)

[a] 7.5 μM porphyrin. [b] nm. [c] M^{-1} cm^{-1}.

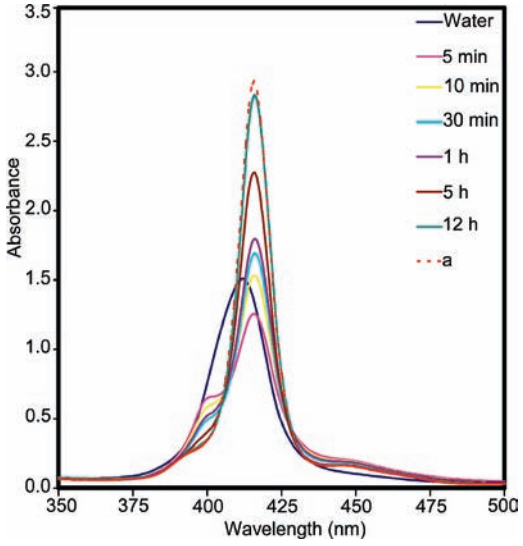

Figure 4. Visible spectrum monitored with time of 7.5 μM [Cu(II)T(*N*-Mepy-4-$CH_2(CH_3)NSO_2Ar$)P]Cl_4 (Cu(II)**6**) in 1 M SDS. Also shown are the spectrum in water and that in 1 M SDS but prepared with a dilute solution of the porphyrin (spectrum a, red dashed line).

to the λ_{So} at 410 nm of an aqueous red solution of Cu(II)**6** (no added salt), λ_{So} was shifted slightly to 406 and 403 nm in 10 and 100 mM NaCl solutions, respectively, and ε_{So} decreased (Table 1). A similar comparison of aqueous Zn(II)**6** showed decreases in ε_{So}, but λ_{So} did not change with salt concentration (Table 1). The molar absorptivity of **6**, Cu(II)**6** and Zn(II)**6** in 10 mM NaCl increased with added methanol at least up to 50% methanol. This absorbance increase is attributable to the dissociation of porphyrin aggregates.

The greater width and lower molar absorptivity of the Soret band of Cu(II)**6** compared to that of Cu(II)TMAP [Cu(II)**6**: 410 nm, full width at half-maximum (fwhm) = 22 nm, $\varepsilon_{So} = 2.0 \times 10^5$ M^{-1} cm^{-1} versus Cu(II)TMAP: 411 nm, fwhm = 16 nm, $\varepsilon_{So} = 2.8 \times 10^5$ M^{-1} cm^{-1}] in aqueous solution indicate that Cu(II)**6** aggregates significantly. Likewise, Zn(II)**6** has fwhm = 14 nm and $\varepsilon_{So} = 2.9 \times 10^5$ M^{-1} cm^{-1}, suggesting that the axial water on Zn as well as other effects of a five-coordinate geometry on the porphyrin structure disfavor stacking. These results suggest that the new cationic porphyrins, even at 7.5 μM, undergo appreciable aggregation and that the aggregated (stacked) Cu(II) porphyrins have relatively blue-shifted Soret bands.

SDS Studies. The λ_{So} and ε_{So} values of Cu(II)**6** in the presence and absence of SDS (Figure 4) are summarized in Table 2. During the first hour after a 1.5 mM stock solution of Cu(II)**6** was added to 1 M SDS to make a 7.5 μM solution, the spectra recorded with time (Figure 4) indicated that two forms of the porphyrin were present initially: one form with a blue-shifted λ_{So} at 399 nm and the other form with a red-shifted λ_{So} at 416 nm (when compared to λ_{So} at 410 nm in water). The facts that the 399 nm Soret band converted completely to the 416 nm Soret band after 12 h and that the intensity of this 416 nm band was high (Figure 4) indicate that Cu(II)**6** is stacked in water and slowly destacks in 1 M SDS.

Table 2. Visible Spectroscopic Data for [Cu(II)T(*N*-Mepy-4-$CH_2(CH_3)$-NSO_2Ar)P]Cl_4 (Cu(II)**6**) in H_2O and 1 M SDS at pH 7.0[a]

	λ_{So}[b] ($10^{-5} \times \varepsilon_{So}$)[c]	
time	H_2O	1 M SDS
5 min	410 (2.0)	416 (1.6), 399 (1.0)
10 min		416 (2.1), 399 (1.1)
30 min		416 (2.4), 399 (1.0)
1 h		416 (2.5), 399 (1.0)
12 h		416 (3.8)

[a] 7.5 μM porphyrin. [b] nm. [c] M^{-1} cm^{-1}.

To test this interpretation, the concentrated stock solution of Cu(II)**6** was diluted to 15 μM. Equal volumes of this dilute solution and a 2 M SDS solution were mixed, producing final concentrations of 1 M SDS and 7.5 μM Cu(II)**6**. The absorption spectrum recorded immediately shows only the red-shifted 416 nm band (Figure 4). This intense band is very similar to the band observed in the experiment described in the previous paragraph. These observations are consistent with a high degree of aggregation of Cu(II)**6** in water, especially at high concentrations, and with SDS causing disaggregation of Cu(II)**6**. (When the Cu(II)**6** is less stacked, the Soret band is red-shifted.)

When a 1.5 mM stock solution of Cu(II)**6** was added to 0.1 M SDS to make a 7.5 μM solution, the spectrum recorded with time (Supporting Information, Figure S11) indicated that both the 399 and 416 nm bands were present, suggesting coexistence of two forms. The two bands remained even after 12 h. This fact suggests that, in contrast to 1 M SDS, 0.1 M SDS does not cause complete disaggregation of the stacked positively charged porphyrin cation. SDS has negative charge, favoring stacking (aggregation) and hydrophobic character, favoring destacking. Evidently, the hydrophobic capacity of 0.1 M SDS is not sufficient to offset the effect of the negative charge.

DNA-Binding Studies. Several methods were used to evaluate DNA binding. We assessed how the Soret band position and intensity changed on DNA addition. Hypochromicity (%*H*) is defined here as $[(A_o - A_s)/A_o] \times 100\%$, where A_o and A_s are the absorbance values at λ_{So} in the absence and presence of CT DNA, respectively (a negative %*H* indicates *hyper*chromicity). Because both CT DNA and the free porphyrin have no CD band in the visible region, the only CD signal observed in this region is the induced CD signal of the bound porphyrins. Viscosity measurements are also useful because intercalation of a cation into DNA has a measurable effect on solution flow properties.[20] A fixed concentration (75 μM) of sonicated CT DNA was maintained as the concentration of several porphyrins in 100 mM NaCl was increased

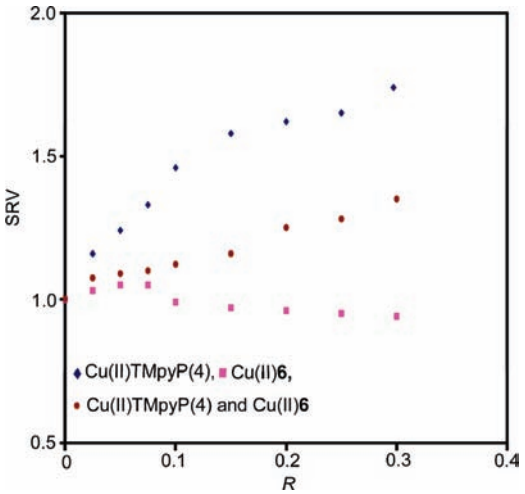

Figure 5. Plot of SRV versus R for the addition of metalloporphyrins to solutions of CT DNA (75 μM, 100 mM NaCl, pH 7.0).

(Figure 5). The SRV increased with addition of the intercalating Cu(II)TMPyP(4). For Cu(II)TMAP the SRV first increased slightly at low R, but leveled off after $R = 0.15$. The addition of Cu(II)**6**, Zn(II)**6**, or Cu(II)**7** to CT DNA caused changes in SRV similar to those observed for the non-intercalating Cu(II)TMAP (Figures 5 and S1). Viscosity experiments were used to determine if Cu(II)**6** binds DNA competitively with Cu(II)TMpyP(4). At different R values (0.025, 0.1, 0.2, and 0.3) with equimolar amounts of the two porphyrins, the SRV values found (1.08, 1.12, 1.25, and 1.35) were smaller than the respective values (1.16, 1.46, 1.62, and 1.74) for Cu(II)TMpyP(4) alone, Figure 5 and Supporting Information, Figure S1.

DNA Binding of [Cu(II)T(*N*-Mepy-4-$CH_2(CH_3)NSO_2Ar$)P]Cl_4 (Cu(II)6). The Cu(II)**6**−CT DNA visible studies are summarized in Table 3. After addition of CT DNA, the spectrum of Cu(II)**6** exhibited two Soret components. The red-shifted component (at 420 nm) in both 10 mM and 100 mM NaCl solutions (Table 3, Figure 6, and Supporting Information, Figure S2) is indicative of an unstacked bound form. As more CT DNA was added (as R changed from 0.25 to 0.005), the intensity of the long-wavelength component increased at the expense of the shorter-wavelength component. *Hyper*chromicity of the Soret band indicates unstacking of Cu(II)**6**.

The overall shape of the CD spectrum of Cu(II)**6** was independent of NaCl concentration. The binding of Cu (II)**6** to CT DNA for all R values induced a CD spectrum with a positive feature at ~415 nm (+exc) and a weak negative feature (-s) at ~433 nm (Table 4, Figure 7, and Supporting Information, Figure S3). The intensity of the positive band increased with increasing CT DNA concentration (decreasing R), while that of the negative feature decreased. At $R = 0.005$ in 10 mM NaCl the CD signal of Cu(II)**6** with CT DNA reached its maximum value (molar ellipticity ([Θ]) = 4.9×10^4 deg cm^2 dmol^{-1}). These results and similar data for 100 mM NaCl are consistent with non-stacking or weakly stacking outside binding.

DNA Binding of [Zn(II)T(*N*-Mepy-4-$CH_2(CH_3)NSO_2Ar$)P]Cl_4 (Zn(II)6). Addition of CT DNA to a solution of Zn(II)**6** in 10 mM and 100 mM NaCl solutions caused a 3 nm red shift in λ_{So} at all R values (Supporting Information, Table S1). At the lowest DNA concentration, only small changes in Soret band intensity in both 10 mM and 100 mM NaCl solutions were observed (Supporting Information, Table S1 and Figures S6 and S7). At the highest DNA concentration ($R = 0.005$), significant *hyper*chromicity was observed in 10 mM (%$H = -61$) and 100 mM (%$H = -87$) NaCl solutions (Supporting Information, Table S1 and Figures S4 and S5). At low R values, an induced CD signal (+exc at ~420 nm) was observed (Supporting Information, Table S2 and Figures S6 and S7). As concluded for Cu(II)**6**, these results are consistent with non-stacking or weakly stacking outside binding.

Table 3. Visible Spectroscopic Data for [Cu(II)T(*N*-Mepy-4-$CH_2(CH_3)NSO_2Ar$)P]Cl_4 (Cu(II)**6**) in the Presence of CT DNA at pH 7.0[a]

	10 mM NaCl			100 mM NaCl		
R	λ_{So}[b]	$10^{-5}\times\varepsilon_{So}$[c]	$\Delta\lambda$[b] (%H)	λ_{So}[b]	$10^{-5}\times\varepsilon_{So}$[c]	$\Delta\lambda$[b] (%H)
0	406	1.6		403	1.1	
0.25	404	1.2	−2 (25)	403	1.0	0 (9)
	420	1.3	14 (19)	420	1.2	17 (−9)
0.05	404	1.1	−2 (31)			
	420	1.6	14 (0)	420	1.4	17 (−27)
0.01	404	1.0	−2 (38)			
	420	1.6	14 (0)	420	2.2	17 (−100)
0.005	404	1.0	−2 (38)			
	420	1.8	14 (−13)	420	2.4	17 (−118)

[a] 7.5 μM porphyrin. [b] nm. [c] M^{-1} cm^{-1}.

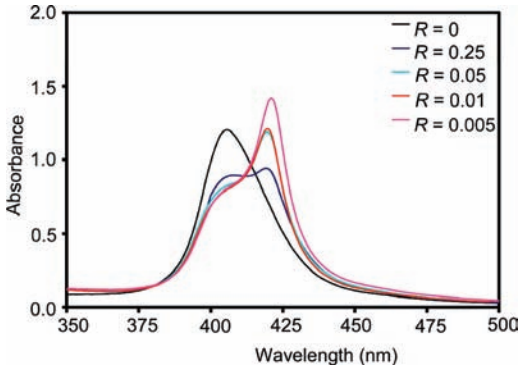

Figure 6. Effect of CT DNA on the visible spectrum of [Cu(II)T(*N*-Mepy-4-$CH_2(CH_3)NSO_2Ar$)P]Cl_4 (Cu(II)**6**, 7.5 μM) at various R values (10 mM NaCl, pH 7.0).

DNA Binding of [Cu(II)T($Et_3NCH_2CH_2$)$_2NSO_2Ar$)P]Cl_8 (Cu(II)7). Addition of CT DNA to Cu(II)**7** caused 7 and 11 nm red shifts of λ_{So} in 10 mM and 100 mM NaCl solutions, respectively (Table 5). At the highest concentration of DNA ($R = 0.005$), *hyper*chromicity was observed (Table 5, Figures 8, and Supporting Information, Figure S8). An induced CD signal (+exc at ~415 nm, -s at ~430 nm) was observed upon addition of CT DNA (Table 6). The intensity of these features generally decreased with an increase in DNA concentration (Table 6, Figure 9, and Supporting Information, Figure S9). As concluded for Cu(II)**6**, these results are consistent with non-stacking or weakly stacking outside binding.

DNA-Binding Studies of Porphyrins with Different Peripheral Groups. The λ_{So} of solutions of both **1** ([T(*N*-Mepy-2-CH_2(H)NSO_2Ar)P]Cl_4) and **5** ([T(*N*-Mepy-2-$CH_2(CH_3)NSO_2Ar$)P]Cl_4) in 10 mM NaCl was at

Table 4. Effect of NaCl Concentration on the CD Spectrum of [Cu(II)T(*N*-Mepy-4-$CH_2(CH_3)NSO_2Ar$)P]Cl_4 (Cu(II)**6**) in the Presence of CT DNA at pH 7.0[a]

	10 mM NaCl				100 mM NaCl			
R	λ_{+exc}[b]	$10^{-4} \times [\Theta]_{+exc}$[c]	λ_{-s}[b]	$10^{-4} \times [\Theta]_{-s}$[c]	λ_{+exc}[b]	$10^{-4} \times [\Theta]_{+exc}$[c]	λ_{s}[b]	$10^{-4} \times [\Theta]_{-s}$[c]
0.25	413	2.3	433	−1.2	412	1.9	433	−0.5
0.05	414	3.2	433	−0.7	416	3.8	434	−0.2
0.01	415	3.6	433	−0.6	417	4.3	434	−0.5
0.005	416	4.9	433	−0.3	414	2.3	434	−0.2

[a] 7.5 μM porphyrin. [b] nm. [c] deg cm^2 $dmol^{-1}$.

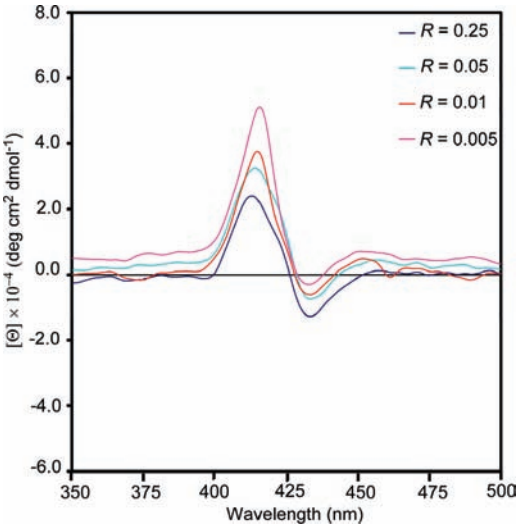

Figure 7. CT DNA-induced CD spectra of [Cu(II)T(*N*-Mepy-4-$CH_2(CH_3)NSO_2Ar$)P]Cl_4 (Cu(II)**6**, 7.5 μM) at various *R* values (10 mM NaCl, pH 7.0).

Table 5. Visible Spectroscopic Data for [Cu(II)T($Et_3NCH_2CH_2)_2NSO_2Ar$)P]Cl_8 (Cu(II)**7**) in the Presence of CT DNA at pH 7.0[a]

	10 mM NaCl			100 mM NaCl		
R	λ_{So}[b]	$10^{-5} \times \varepsilon_{So}$[c]	$\Delta\lambda$[b] (%*H*)	λ_{So}[b]	$10^{-5} \times \varepsilon_{So}$[c]	$\Delta\lambda$[b] (%*H*)
0	414	2.3		409	2.2	
0.25	421	2.0	7 (13)	420	2.4	11 (−9)
0.05	421	2.2	7 (4)	420	2.8	11 (−27)
0.01	421	2.4	7 (−4)	420	3.0	11 (−36)
0.005	421	2.7	7 (−17)	420	3.2	11 (−46)

[a] 7.5 μM porphyrin. [b] nm. [c] M^{-1} cm^{-1}.

414 nm (Supporting Information, Table S3). The addition of CT DNA at a low DNA concentration (*R* = 0.25) to **1** and **5** led to red-shifted and blue-shifted (5 nm) bands and hypochromicity. At the higher DNA concentration (*R* = 0.005), the same two bands were observed (%*H* = 52 and 7 for **1** and %*H* = 54 and 15 for **5**, Supporting Information, Table S3). The binding of CT DNA to both porphyrins induced a positive CD feature (Supporting Information, Table S4). As more CT DNA was added (as *R* changed from 0.25 to 0.005), the intensity of these positive features increased (Supporting Information, Table S4). Visible and CD spectral changes for **4** ([T($Me_3NCH_2CH_2$(H)-NSO_2Ar)P]Cl_4) in 10 mM NaCl (Supporting Information, Tables S3 and S4) were similar to those for **1** and **5**. The spectral features of the porphyrins described in this subsection are consistent with a combination of weakly

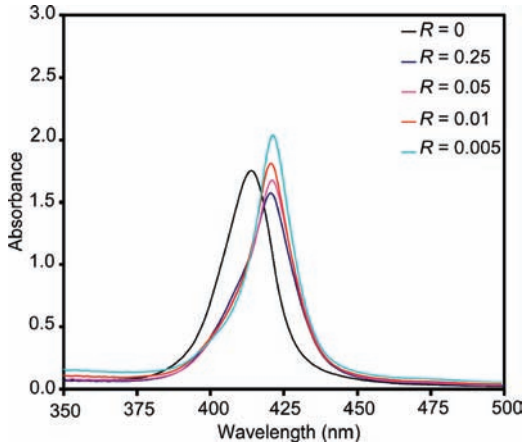

Figure 8. Effect of CT DNA on the visible spectrum of [Cu(II)T-($Et_3NCH_2CH_2)_2NSO_2Ar$)P]Cl_8 (Cu(II)**7**, **7**.5 μM) at various *R* values (10 mM NaCl, pH 7.0).

stacked and unstacked outside binding rather than with intercalation.

Fluorescence Spectroscopy. The fluorescence spectrum of the metal-free porphyrin, [T(*N*-Mepy-4-$CH_2(CH_3)$-NSO_2Ar)P]Cl_4 (**6**), in 10 mM NaCl shows two emission maxima at 656 nm [Q(0,0) band] and at ~700 nm [Q(0,1) band] (Figure 10); the band assignment follows that used for other porphyrins.[49] The two bands shifted (656 nm band slightly, ~700 nm band significantly), and the intensity decreased significantly (by 34% and ~60%, respectively, Figure 10) upon the addition of a small amount of DNA (*R* = 0.25). The decrease in fluorescence intensity of **6** is attributed to the proximity of the neighboring porphyrins, which are self-stacked when bound to DNA.[50] Further addition of CT DNA led to increases in intensity. The final value (*R* = 0.005) was ~1.2 times those found before DNA addition. We attribute these changes to conversion of the unbound porphyrin aggregates initially present first to bound aggregates (Figure 2, right) and then to the bound monomer form at high DNA concentration (Figure 2, middle).[50]

Discussion

Our primary interests were to determine how the new water-soluble cationic porphyrins and metalloporphyrins prepared in this work bound to DNA, either as intercalators or outside-binders, and to use the results to gain further insight into important features that favor intercalation of

(49) Kano, K.; Takei, M.; Hashimoto, S. *J. Phys. Chem.* **1990**, *94*, 2181–2187.
(50) Nyarko, E.; Hanada, N.; Habib, A.; Tabata, M. *Inorg. Chim. Acta* **2004**, *357*, 739–745.

Table 6. Effect of NaCl Concentration on the CD Spectrum of $[Cu(II)T(Et_3NCH_2CH_2)_2NSO_2Ar)P]Cl_8$ (Cu(II)**7**) in the Presence of CT DNA at pH 7.0[a]

	10 mM NaCl				100 mM NaCl			
R	λ_{+exc}[b]	$10^{-4} \times [\Theta]_{+exc}$[c]	λ_{-s}[b]	$10^{-4} \times [\Theta]_{-s}$[c]	λ_{+exc}[b]	$10^{-4} \times [\Theta]_{+exc}$[c]	λ_{s}[b]	$10^{-4} \times [\Theta]_{-s}$[c]
0.25	414	3.9	428	−3.0	414	2.1	430	−1.5
0.05	415	2.6	430	−0.7	414	1.2	430	−0.7
0.01	415	1.8	429	−0.9	414	1.5	430	−0.5
0.005	415	1.6	429	−0.8	419	0.8	436	−0.5

[a] 7.5 μM porphyrin. [b] nm. [c] deg cm^2 dmol^{-1}.

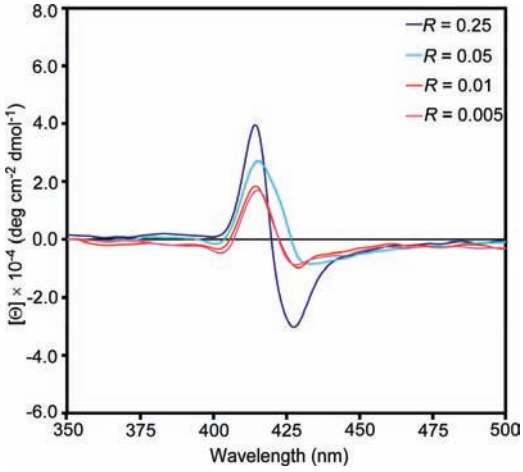

Figure 9. CT DNA-induced CD spectra of $[Cu(II)T(Et_3NCH_2CH_2)_2NSO_2Ar)P]Cl_8$ (Cu(II)**7**, 7.5 μM) at various R values (10 mM NaCl, pH 7.0).

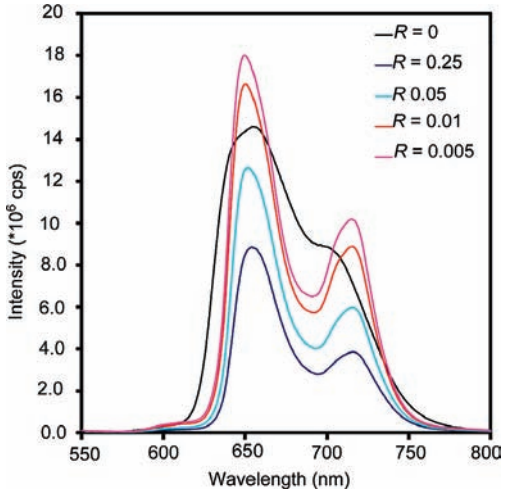

Figure 10. Effect of CT DNA on the fluorescence spectrum of $[T(N\text{-Mepy-4-}CH_2(CH_3)NSO_2Ar)P]Cl_4$ (**6**, 7.5 μM) at various R values (10 mM NaCl, pH 7.0).

cationic porphyrins. Experimental evidence useful for determining if a porphyrin intercalates and our evidence establishing that the new porphyrins do not intercalate will be discussed first. Next we discuss the factors that our work indicates are important for intercalation of known porphyrin intercalators. Finally, we shall discuss briefly the nature of the DNA outside binding of the new porphyrins.

Experimental Criteria for Porphyrin Intercalation into DNA. Experimental observations indicating intercalative binding include changes in the Soret region of spectra, namely, a large red shift (~15 nm), a large hypochromicity (~30%), and a negative induced CD signal. These spectroscopic parameters tend to vary over a narrower range than those found for outside binders (see below). Perhaps the most characteristic spectral feature is the negative induced CD signal; typical magnitudes found are about -5×10^4 (deg cm^2/dmole).[5,31,37,38,51] However, perhaps the best procedure to assess DNA binding mode is to measure SRV. Porphyrins known to intercalate (e.g., Cu(II)TMpyP(4)[52]) increase the SRV of DNA solutions.[31]

Evidence That New Porphyrins Are Not Intercalators. No increase in DNA solution viscosity was observed for Cu(II)**6**, Zn(II)**6**, and Cu(II)**7** (Figure 5 and Supporting Information, Figure S1). The SRV values of Cu(II)**6**, Zn(II)**6**, and Cu(II)**7** were comparable to that of Cu(II)-TMAP, a non-intercalator.[53] The absence of an increase in SRV demonstrates that these new porphyrins are outside binders. At the same ratio of total Cu(II) porphyrin to DNA, lower SRV values were found in the presence of both $[Cu(II)T(N\text{-Mepy-4-}CH_2(CH_3)NSO_2Ar)P]Cl_4$ and Cu(II)-TMpyP(4) than in the presence of Cu(II)T-MpyP(4) alone (Figure 5). This finding indicates that $[Cu(II)T(N\text{-Mepy-4-}CH_2(CH_3)NSO_2Ar)P]Cl_4$ competes for DNA with Cu(II)TMpyP(4), which has a DNA binding constant of $\sim 10^7$ M^{-1}.[54] Therefore, because all the new porphyrins are similar, we expect that all are tight outside binders to DNA, and we turn our attention to comparing the features of the new porphyrins versus intercalating porphyrins to identify important features for intercalation.

Properties of Porphyrins Favoring Intercalation. On the basis of our past work and that of others,[1,19−21,29,52,55,56] we can conclude that for intercalation the porphyrin peripheral groups should be *N*-alkyl pyridinium groups and that the porphyrin core of the metalloporphyrins with these groups must lack axial ligands (e.g., Cu(II)-TMpyP(4)) or have dissociable axial ligands (e.g., i(II)-TMpyP(4)).[1,19,22,56] In general, the length of the *N*-alkyl group does not appear to be important;[22,31−34,57,58]

(51) McMillin, D. R.; Shelton, A. H.; Bejune, S. A.; Fanwick, P. E.; Wall, R. K. *Coord. Chem. Rev.* **2005**, *249*, 1451–1459.
(52) Strickland, J. A.; Marzilli, L. G.; Wilson, W. D. *Biopolymers* **1990**, *29*, 1307–1323.
(53) Pasternack, R. F.; Ewen, S.; Rao, A.; Meyer, A. S.; Freedman, M. A.; Collings, P. J.; Frey, S. L.; Ranen, M. C.; de Paula, J. C. *Inorg. Chim. Acta* **2001**, *317*, 59–71.
(54) Strickland, J. A.; Marzilli, L. G.; Gay, K. M.; Wilson, W. D. *Biochemistry* **1988**, *27*, 8870–8878.
(55) Pasternack, R. F.; Brigandi, R. A.; Abrams, M. J.; Williams, A. P.; Gibbs, E. J. *Inorg. Chem.* **1990**, *29*, 4483–4486.
(56) Strickland, J. A.; Marzilli, L. G.; Wilson, W. D.; Zon, G. *Inorg. Chem.* **1989**, *28*, 4191–4198.
(57) Yue, K. T.; Lin, M. F.; Gray, T. A.; Marzilli, L. G. *Inorg. Chem.* **1991**, *30*, 3214–3222.
(58) Bordbar, A. K.; Mohammadi, K.; Keshavarz, M.; Dezhampanah, H. *Acta Chim. Slov.* **2007**, *54*, 336–340.

however, the *N*-alkylpyridinium group must link to the porphyrin core via the 4- or 3- position of the pyridyl ring (not via the 2- position). This latter requirement has three implications: First, and most important, this requirement indicates that a relatively planar structural unit involving the pyridinium group and the adjacent portion of the porphyrin ring must be achieved. Second, the overall electronic nature of the directly attached pyridinium group and the porphyrin core appear to be important. Third, and less obvious, the separation between the charged nitrogens of the pyridinium groups may need to fall within a required range. These distances can be shorter (~6.5 Å) for TMpyP(2). The latter two aspects can be assessed with the results from our current work.

A recent paper contained a comparison of TMpyP(4) and its analogue with a 4-phenylene group inserted between the *N*-methylpyridinium group and the porphyrin core (B-TMpyP(4), Figure 1).[59] The latter compound does not intercalate. In TMpyP(4) the distances between the N's of the *N*-Mepy groups are 11 Å (cis) and 16 Å (trans), whereas for B-TMpyP(4) these distances between the N's of the 4-C_6H_4−*N*-Mepy groups are 19 Å (cis) and 27 Å (trans). This comparison suggests both that the separation between the charged nitrogens must be smaller and that, as mentioned above, the pyridinium group must be directly attached to the porphyrin core. The recent work of the McMillin laboratory showing that triD4 (Figure 1) intercalates indicates that a separation of 16 Å allows intercalation. This separation corresponds somewhat to the cis distance in B-TMpyP(4). McMillin et al. showed that when bulk is present cis to the pyridinium groups (MetriD4), such larger porphyrins do not intercalate as well as the original smaller porphyrin.[38] The 4-C_6H_4-*N*-Mepy group is large and projects out in a rigid manner. Other relatively large pyridinium porphyrins that intercalate have cis pyridinium groups with flexible *N*-alkyl substituents,[22,31] and this flexibility might allow the alkyl group to adopt an orientation that does not inhibit intercalation. In contrast, we believe that the rigid 4-C_6H_4-*N*-Mepy groups of B-TMpyP(4) do not allow the meso peripheral groups to avoid the steric clashes. Unlike B-TMpyP(4), the [T(*N*-Mepy-4-$CH_2(CH_3)NSO_2$Ar)P]-Cl_4 porphyrins studied here are quite conformationally flexible. The various conformations can place the pyridinium groups in positions covering a range of distances from 9 Å (cis) to 25 Å (trans). These distances encompass those in pyridinium porphyrins for which intercalation has been found. However, the new porphyrins do not intercalate. This finding refines further the requirements for a porphyrin to be an intercalator and indicates that direct attachment of the pyridinium group to the porphyrin core is a very favorable and probably necessary feature for intercalation to occur. We believe the steric and electronic features of the combined pyridinium group and adjacent portions of the porphyrin core facilitate intercalation.

Stacking of Cationic Porphyrins under Aqueous Conditions. In the absence of DNA, many porphyrins undergo self-stacking in water.[39,60−64] The Soret bands of the face-to-face (H) and edge-to-edge (J) type stacked porphyrins are respectively blue-shifted and red-shifted.[60,63] The H-type stacking involves considerable overlap of the porphyrin cores, whereas J-type stacking can be viewed as a slippage of the porphyrin cores so that there is less overlap.[60] The electronic spectra are also influenced by the way the porphyrins align with respect to each other because alignment influences the relative orientation of the transition moments.[63] It was not our objective to analyze in depth this very complicated stacking process. Rather, our goal was to determine qualitatively the relative importance of stacking for the unbound porphyrin because stacking influences the electronic spectra, and understanding this influence is useful in assessing spectral changes accompanying binding.

For types of cationic porphyrins usually studied, self-stacking upon DNA binding is normally accompanied by hypochromicity, broadening, and/or a shift in λ_{So}.[4−7,20,29,33] Self-aggregation of cationic porphyrins is believed to be responsible for the large hypochromicities (50−65%) observed in high salt concentrations.[29,33,39] From data in previous studies[29,61] the spectral changes indicate that TMAP and *trans*-P(4) in the presence of salt exist as H- and J-type aggregates, respectively.

Properties of the New Cationic Porphyrins in the Absence of DNA. We investigated the behavior of selected new porphyrins under aqueous conditions. The addition of NaCl to a solution of [Cu(II)T(*N*-Mepy-4-$CH_2(CH_3)$-NSO_2Ar)P]Cl_4 (Cu(II)**6**) affected the Soret band, causing a blue shift, a broadening, and a decrease in the intensity (%H = 70 at 3.0 M NaCl, Supporting Information, Figure S10). These changes in the visible spectrum indicate that Cu(II)**6** undergoes substantial self-stacking and that the aggregates are of the H-type. Even in water, Cu(II)**6** gives evidence for stacking and the stacking increases under the low salt conditions used here. The literature indicates TMpyP(4) exists as the monomer in water even in the presence of inorganic salts.[24,65] Indeed, we compared aqueous and 200 mM NaCl solutions of TMpyP(4) and found that the Soret band (421 nm) did not shift and there was little change in intensity (%H = 3). In the same type of experiment but with Cu(II)**6** the Soret band showed a blue shift (9 nm) and %H = 45. Thus, Cu(II)**6** has a greater propensity to stack than TMpyP(4).

Addition of SDS to a solution of Cu(II)**6** produced a visible spectrum with two Soret bands at 399 and 416 nm. At low SDS concentration (0.1 M) the two bands were observed even after 12 h (Supporting Information, Figure S11). After 12 h in a 1 M solution of SDS the blue-shifted Soret band at 399 nm converted completely to the 416 nm band (red-shifted by 4 nm, an indication of a J-type aggregate). The intensity of this band increased with time (%H = −90 after 12 h, Figure 4). For TMpyP(4) at

(59) Lee, M. J.; Jin, B.; Lee, H. M.; Jung, M. J.; Kim, S. K.; Kim, J. M. *Bull. Korean Chem. Soc.* **2008**, *29*, 1533–1538.
(60) de Miguel, G.; Perez-Morales, M.; Martin-Romero, M. T.; Munoz, E.; Richardson, T. H.; Camacho, L. *Langmuir* **2007**, *23*, 3794–3801.
(61) Dixon, D. W.; Steullet, V. *J. Inorg. Biochem.* **1998**, *69*, 25–32.
(62) Maiti, N. C.; Mazumdar, S.; Periasamy, N. *J. Phys. Chem. B* **1998**, *102*, 1528–1538.
(63) Wang, Y. T.; Jin, W. J. *Spectrochim. Acta, Part A* **2008**, *70*, 871–877.
(64) Martin, M. T.; Prieto, I.; Camacho, L.; Mobius, D. *Langmuir* **1996**, *12*, 6554–6560.
(65) Pasternack, R. F.; Centuro, G. C.; Boyd, P.; Hinds, L. D.; Huber, P. R.; Francesconi, L.; Fasella, P.; Engasser, G.; Gibbs, E. *J. Am. Chem. Soc.* **1972**, *94*, 4511–4517.

neutral pH, SDS produced no spectral shifts and thus the aggregate type could not be assigned as H- or J-type.[62]

The Soret band of octacationic [Cu(II)T(Et_3-$NCH_2CH_2)_2NSO_2Ar$)P]Cl_8 (Cu(II)**7**) in water (λ_{So} = 414 nm) was much sharper than that of Cu(II)**6**, indicating that Cu(II)**7** is less aggregated than Cu(II)**6** in water. Upon addition of salt, the Soret band of Cu(II)**7** became less intense and broader, and these effects increased with increasing salt (Supporting Information, Figure S12). These characteristics indicate that Cu(II)**7** undergoes self-stacking with an increase in salt concentration. At 3.0 M NaCl, the %*H* value of 57 is less than that of Cu(II)**6**. All results indicate that (because of its high charge) stacking of Cu(II)**7** is lower than that of Cu(II)**6**.

In aqueous 10 and 100 mM NaCl, the solution conditions used here for DNA binding studies, the Soret band of Cu(II)**6**, Cu(II)**7** and also Zn(II)**6** (Figure 3) gave evidence for aggregation (Table 1). Upon DNA addition (see below), the Soret bands of these porphyrins shifted to the red and sharpened. The significant *hyper*chromicity and the red shift of the Soret bands are indicative of porphyrin binding to DNA as non-self-stacking outside binders.[21,28,31,66] Such changes must be assessed in the context of the degree of aggregation with stacking of the unbound porphyrin. For example, the extent of the *hyper*chromicity on DNA binding is less for Cu(II)**7** than for Cu(II)**6** because Cu(II)**7** is already less self-stacked than Cu(II)**6** prior to DNA binding. Thus, the DNA-bound Cu(II)**7** is not stacked (see below).

Outside Binding to DNA by Porphyrins. Porphyrins that induce no increase in the SRV of linear DNA are outside binders. The type of outside binding can be evaluated by observation of features of the induced CD signal. In addition, the Soret region of the visible spectrum undergoes changes. Because outside binding depends on a number of variables such as salt, ratio of porphyrin to the DNA, DNA base pair composition, and so forth, and because there can be combinations of coexisting outside binding modes, simple spectral signatures are difficult to define and categorize. In addition, because self-stacking often occurs and the self-stacking can itself change with the various conditions, it is not a simple matter to define precisely the binding. To illustrate the effects on CD and Soret spectra on porphyrin outside binding to DNA, we consider three limiting cases (Figure 2, middle and right), namely, no self-stacking with the porphyrin core close to the DNA, no self-stacking with the core somewhat further and tumbling anisotropically, and extensive self-stacking.

Each of the three cases gives a distinct induced CD signal. A relatively unstacked outside-bound porphyrin will typically have a non-conservative positive CD signal with an intensity for [Θ] = $\sim 1 \times 10^5$ deg cm^2 dmol^{-1}.[21,31] One system with this type of binding is TMpyP(4)−[poly(dA-dT)]$_2$.[21,31] We believe that TMpyP(2) is an example of a porphyrin that exhibits tumbling anisotropically. No appreciable induced CD signal was observed.[21] Conservative CD signals (in some cases strong) are indicative of outside binding with self-stacking.[4,5,30,33,35−37,67] Although the negative and positive features for the conservative signal detected are often not much stronger than the single prominent feature of an unstacked porphyrin, porphyrins with tentacle arms (e.g., T*θ*OPP) offer an example of extensive self-stacking on DNA with both positive and negative features [Θ] having an absolute magnitude 10 times greater than normal, with values of $\sim 10^6$ deg cm^2 dmol^{-1}.[33]

The Soret band is also useful for assessing stacking. As mentioned above, hyperchromicity is most reliably indicative of outside-bound unstacked porphyrins. Previously studied porphyrins (Mn(III)TMpyP(4) and Co(III)TMpyP(4)) showed small red shifts (5 nm) of the Soret band and significant *hyper*chromicity with CT DNA (−30% and −27%, respectively).[21] Outside binding with porphyrin stacking produces variable effects on the Soret band. A moderate (9 nm) red shift of λ_{So}, along with less than 30% hypochromicity[4,5] has been observed, but a large (25−30 nm) red shift[29] with large (∼60%) hypochromicity has also been observed.[29,30,33,34,67]

[Cu(II)T(*N*-Mepy-4-$CH_2(CH_3)NSO_2Ar$)P]Cl_4 (Cu(II)-6) and [Zn(II)T(*N*-Mepy-4-$CH_2(CH_3)NSO_2Ar$)P]Cl_4 (Zn (II)6). Visible and CD spectroscopic results for Cu(II)**6** and Zn(II)**6** are consistent with both being non-stacking outside binders. After addition of CT DNA to Cu(II)**6** and Zn(II)**6**, a red-shifted Soret band component was evident. Large *hyper*chromicities (Table 3) of up to −118% for Cu(II)**6** were observed. At all *R* values, a positive induced CD band (Figure 7 and Supporting Information, Figure S3) for Cu(II)**6** was observed at ∼416 nm, indicative of outside binding. Likewise, Zn(II)**6** exhibited a positive CD band (Supporting Information, Figures S6 and S7), a red shift (3 nm) and *hyper*chromicity (%*H* as large as −87) of the Soret band (Supporting Information, Table S1). We conclude that both Cu(II)**6** and Zn(II)**6** are non-stacking outside binders.

Another method for assessing binding mode is fluorescence. Porphyrins exhibit reduced fluorescence intensity at high *R* followed by increase in fluorescence intensity as *R* decreases. However, Cu(II)**6** does not have usable fluorescence intensity. Because the metal-free porphyrin, [T(*N*-Mepy-4-$CH_2(CH_3)NSO_2Ar$)P]Cl_4 (**6**), exhibits spectral features on addition of CT DNA similar to those found for Cu(II)**6**, we studied **6**. The fluorescence intensity of **6** first decreased and then increased as *R* decreased (Figure 10), another finding indicating that non-stacking outside binding at low *R*.[33,50] In view of the similar structures and visible spectral behavior of **6** and Cu(II)-**6**, the fluorescence data support the other results indicating that Cu(II)**6** is a non-self-stacking outside binder.

[Cu(II)T($Et_3NCH_2CH_2)_2NSO_2Ar$)P]Cl_8 (Cu(II)7). Cu-(II)**7** is also a non-stacking outside binder as evidenced by a small red shift (7−11 nm) and (except at high *R* and low salt) *hyper*chromicity of the Soret band (Table 5, Figures 8, and Supporting Information, Figure S8). The highest *hyper*chromicity observed for Cu(II)**7** (%*H* = −46) was much lower than that of Cu(II)**6** and Zn(II)**6** because the unbound Cu(II)**7** is not significantly self-stacked. For the Cu(II)**7**-DNA adduct at

(66) Lugo-Ponce, P.; McMillin, D. R. *Coord. Chem. Rev.* **2000**, *208*, 169–191.

(67) Hudson, B. P.; Sou, J.; Berger, D. J.; McMillin, D. R. *J. Am. Chem. Soc.* **1992**, *114*, 8997–9002.

R = 0.005 (100 mM), the magnitude of ε_{So} ($3.2 \times 10^5\ M^{-1}\ cm^{-1}$) is typical of a non-stacking outside binder.

Other Porphyrins. [T(*N*-Mepy-2-CH_2(H)NSO_2Ar)P]-Cl_4 (**1**) and [T(*N*-Mepy-2-CH_2(CH_3)NSO_2Ar)P]Cl_4 (**5**) have *N*-Mepy groups similar to those in TMpyP(2), but unlike TMpyP(2), their interaction with CT DNA led to a red shift (8 nm) of the Soret band, *hyper*chromicity, and a positive CD feature (Supporting Information, Tables S3 and S4). These results indicate that **1** and **5** are non-stacking outside binders. The Soret band of TMpyP(2) was unaffected by interaction with CT DNA, and no *hyper*chromicity or CD signal was observed.[21] Because the *N*-Mepy groups of TMpyP(2) are close to the porphyrin core, steric hindrance between the *N*-Me group and the pyrrole protons prevents the pyridinium group from rotating to become coplanar with the porphyrin core, thus hindering intercalation.[21] However, we suggest that another effect of the *N*-Mepy groups linked via the 2-position in TMpyP(2) is to keep the porphyrin core from interacting tightly with DNA. In this situation, we believe that the porphyrin is tumbling anisotropically (Figure 2). Compared to TMpyP(2), the *N*-Mepy groups of [T(*N*-Mepy-2-CH_2(H)NSO_2Ar)P]Cl_4 and [T(*N*-Mepy-2-CH_2(CH_3)NSO_2Ar)P]Cl_4 are far from the porphyrin core and thus do not inhibit the porphyrin core from approaching the DNA closely. We propose proximity is needed for a CD signal to be induced.

Conclusions

T(*N*-Mepy-4-CH_2(CH_3)NSO_2Ar)P]Cl_4 (**6**), [Cu(II)T(*N*-Mepy-4-CH_2(CH_3)NSO_2Ar)P]Cl_4 (Cu(II)**6**), [Zn(II)T(*N*-Mepy-4-CH_2(CH_3)NSO_2Ar)P]Cl_4 (Zn(II)**6**), and [Cu(II)T-($Et_3NCH_2CH_2$)$_2NSO_2$Ar)P]Cl_8 (Cu(II)**7**) are tight non-stacking outside binders with CT DNA. Most of these new non-intercalators contain the same 4-substituted *N*-Mepy group as in several known intercalating porphyrins with the *N*-Mepy group directly attached to the porphyrin ring. The 4-substituted *N*-Mepy groups in the new porphyrins can have separations similar to those in intercalating porphyrins, indicating that spacing is not the deciding factor. This finding, along with results on porphyrins with *N*-Mepy groups linked at the 2-position, allowed us to conclude that direct attachment of the *N*-alkylpyridinium groups to the porphyrin ring in such a way that the *N*-alkylpyridinium group can become nearly coplanar with the porphyrin ring is necessary for intercalation to occur.

Our current results showing that [T(*N*-Mepy-4-CH_2(CH_3)-NSO_2Ar)P]Cl_4 and its derivatives are outside binders without self-stacking indicate that their behavior is different from the substantial self-stacking of T*θ*OPP (another porphyrin with an electron-rich core).[33] We attribute the difference in stacking propensity (which we view as a matter of degree, differing in the relative abundance of stacked versus unstacked bound porphyrin) to subtle differences involving the interaction of the charged groups with the DNA. Because the new porphyrins with secondary and tertiary sulfonamide groups bind to DNA in a similar manner, any role of the sulfonamide in hydrogen bonding would be as an H-bond acceptor by the sulfonamide oxygen atoms.

These new porphyrins have various charged groups, but the differences do not affect binding mode. When TMpyP(4) interacts with AT-rich regions of DNA as a non-stacking outside binder, its fluorescence behavior (decrease at high R and increase at low R) is similar to that of **6**. Thus, the porphyrin rings of these two rather different porphyrins probably are positioned relative to DNA in a very similar manner.

The same characteristic binding and spectral changes found for new porphyrins with 4-substituted *N*-Mepy groups were also found for [T(*N*-Mepy-2-CH_2(H)NSO_2Ar)P]Cl_4 and [T(*N*-Mepy-2-CH_2(CH_3)NSO_2Ar)P]Cl_4. These latter contain *N*-Mepy groups attached at the 2-position as in TMpyP(2), a porphyrin that does not exhibit spectral changes upon DNA binding.[21] Our findings indicate that the porphyrin ring of the new porphyrins is close to the DNA when bound in a non-stacking manner (Figure 2). In turn, we conclude that TMpyP(2) tumbles anisotropically, with the porphyrin ring on average farther from the DNA than the porphyrin ring of other porphyrins when these bind outside of DNA (Figure 2).

Acknowledgment. We acknowledge the steadfast interest and encouragement for our studies with porphyrins from the late Professor Peter Hambright of Howard University, and we dedicate this paper and the accompanying paper to his memory. We thank Dr. Steven Soper's research group for the use of their fluorimeter.

Supporting Information Available: Graph of viscosity studies (Figure S1), Figures of visible and CD spectra (Figures S2−S9), visible spectra in different salt concentration (Figures S10 and S12), visible spectra in 0.1 M SDS (Figure S11). Tables of visible and CD data (Tables S1−S4). This material is available free of charge via the Internet at http://pubs.acs.org.